Liquid-liquid phase separation induced auto-confinement

Journal:	*Soft Matter*
Manuscript ID	SM-COM-11-2023-001617.R1
Article Type:	Communication
Date Submitted by the Author:	01-Feb-2024
Complete List of Authors:	Rizvi, Aoon; University of California, Irvine, Department of Chemistry Patterson, Joseph; University of California, Irvine, Department of Chemistry

SCHOLARONE™
Manuscripts

<div style="background:#8BA5BC; color:white;">

COMMUNICATION

</div>

Liquid-liquid phase separation induced auto-confinement

Aoon Rizvi[a], Joseph P. Patterson[a]*

Confinement allows macromolecules and biomacromolecules to attain arrangements typically unachievable through conventional self-assembly processes. In the field of block copolymers, confinement has been achieved by preparing thin films and controlled solvent evaporation through the use of emulsions. A significant advantage of the confinement-driven self-assembly process is its ability to enable block copolymers to form particles with complex internal morphologies, which would otherwise be inaccessible. Here, we show that liquid-liquid phase separation (LLPS) can induce confinement during the self-assembly of a model block copolymer system. Since this confinement is driven by the block copolymers' tendency to undergo LLPS, we define this confinement type as auto-confinement. This study adds to the growing understanding of how LLPS influences block copolymer self-assembly and provides a new method to achieve confinement driven self-assembly.

Confining macromolecules at the nano and microscale has been shown to yield morphologies and arrangements otherwise unattainable.[1–3] Recent studies have also explored the impact of confinement in biological systems,[4,5] including its role in artificial living system development.[6] In polymeric systems, confinement disrupts typical crystallization kinetics and induces preferential crystal orientations.[7–9] In block copolymer systems specifically, 3D confinement is known to encourage the formation of anisotropic oblate particles,[10,11] as well as particles with intricate internal structures, such as helical cavities.[12] Such morphologies are being explored for new applications, such as particle shape dependent rheology,[13] photonics,[14] and templating.[15] The two most commonly used methods to achieve confinement-driven assembly of block copolymer particles are Evaporation-Induced Confinement Assembly (EICA),[16] and the self-organized precipitation (SORP) method.[17] While evaporation of an organic solvent is key to inducing confinement in both methods, the mechanisms are different. EICA achieves 3D confinement by using oil-in-water emulsion systems.[18] In short, an emulsion is created by combining a block copolymer containing organic phase (water-immiscible organic solvent) and a surfactant-containing aqueous phase. This results in the formation of an oil-in-water emulsion in which polymer containing oil droplets are stabilized by surfactants. The system is then heated to evaporate the

organic solvent droplets that contain block copolymer. This evaporation causes the droplet volume to decrease, and the concentration of block copolymers in the droplets to increase. The block copolymers eventually form ordered domains due to microphase separation and confinement from the decreasing droplet volume. The SORP method involves dissolving the polymers in a water miscible organic solvent such as THF, and self-assembly is induced by the addition of a selective solvent like water. The solution is then heated to evaporate the organic solvent, which is key to preparing confined morphologies by the SORP method.[19] In both systems, the evaporation of the organic solvent induces confinement.

The literature on confinement driven block copolymer self-assembly process suggests that confinement is required to form certain morphologies, e.g. hexagonally packed hoops, and continous porous structures. However, these morphologies have also been achieved through conventional solvent switch self-assembly processes without the use of EICA or SORP.[20–22] To the best of our knowledge, no reports have yet been made on the mechanism for the formation of such structures when prepared without 3D soft-confinement.[17–19]

Liquid liquid phase separation (LLPS) has emerged as pathway for the organization of biomacromolecules,[23] biomimetic systems,[24–26] and synthetic systems.[27] Multiple reports have shown that block copolymers undergo liquid-liquid phase separation (LLPS) during the solvent switch self-assembly process.[28–31] LLPS during the solvent switch self-assembly of block copolymer results in the formation of coacervate droplets that act as precursors to the self-assembled particles.[29] This coacervate precursor has been shown to be a critical determinant in the size and morphology of the kinetically trapped self-assembled particles. The coacervate droplets form on the nanoscale at a critical concentration of the selective solvent and grow via coalescence to the microscale. The droplets eventually macrophase separate and form two distinct layers.[29] The rapid growth is due to the dynamic nature of the droplets and no surfactant layers present at the interface to prevent coalescence. As the solvent switch process is continued, the coacervate droplets turn into self-assembled block copolymer particles due to the solvent quality further decreasing for the block copolymers. During this transision the polymer particle become kinetically trapped.[28] The self-assembly initially occurs at the interface of the coacervate droplets as the solvent within the coacervates is expelled out.[28] This

a. *Department of Chemistry, University of California, Irvine, Irvine, CA 92697-2025,*
Irvine, CA 92697-2025

process resembles the confinement procedure in which the oil in water emulsion droplets are evaporated as described above.[16] With this in mind, we hypothesized that for solvent switch processes where LLPS takes place, the formation of the liquid droplet intermediate could result in an auto-confinement driven self-assembly process. We define auto-confinement as a process in which macromolecules experience 3D soft-confinement within the droplets formed by those macromolecules undergoing LLPS. This is different from previously mentioned systems, EICA and SORP, in which confinement is driven by solvent evaporation or the use of an external component. Although the processes by which EICA/SORP confinement and auto-confinement occur are different, we believe the resulting structures should be similar as both process result in block copolymers assembling within a confined volume. If our hypothesis is true, it would provide a plausible mechanism to explain the observation of "confined" morphologies where EICA or SORP methods were not used.[20,31] Furthermore, our hypothesis would provide a new general understanding for how confinement can be achieved through spontaneous processes such as LLPS.

To test the above hypothesis, we sought to find a kinetically trapped polymer system which could assemble via two different pathways depending on the common solvent used (Figure 1). Pathway 1 should self-assemble via a mechanism in which the first phase transition is from the dissolved state to the solid assembled state. Pathway 2 should involve an LLPS event which forms precursor droplets that convert from the liquid state into the self-assembled structures. Our hypothesis is that Pathway 1 should result in the formation of conventional morphologies such as vesicles, whereas pathway two should form confined morphologies with complex internal structures. Based on our previous work,[30] we explored the phase behavior of polystyrene-*block*-polyacrylic acid (PS-*b*-PAA). PS_{200}-*b*-PAA_{35} was synthesized using reversible addition-fragmentation transfer (RAFT) polymerization,[30] where longer hydrophobic blocks were chosen as they are known to promote the formation of vesicles and internally complex structures.[32,33] The phase behavior of PS_{200}-*b*-PAA_{35} was explored by dissolving the polymer in a series of water miscible good solvents and then adding different amounts of water (the selective solvent). The common solvents for this polymer were explored based on previous literature and the starting polymer concentration was 10 mgmL^{-1}.[33–35] As we have shown previously,[29] the phase behavior of the system can be determined through a combination of visual inspection, and optical microscopy (Figure 2). Figure 2a shows photographs of the polymer in 4 different good solvents at the critical water concentration (when the first phase transition event takes place). To test whether the
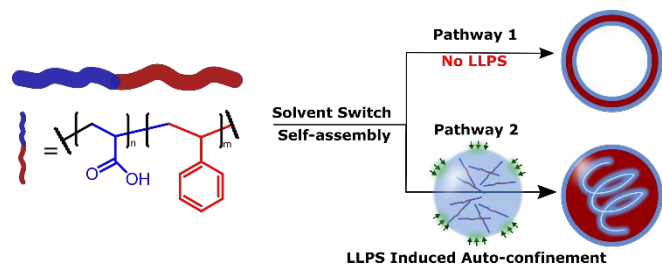

Figure 1. Self-assembly overview of polystyrene-*block*-poly acrylic acid with and without LLPS induced confinement. Pathway 1 proceeds with no confining effects forming vesicles. Pathway 2 proceeds through LLPS intermediates which induce auto-confinement of the block copolymers forming "confined" morphologies.

system underwent LLPS, we centrifuged the sample down which separates the two phases as shown in Figure 2a. The dispersed sample is imaged using an optical microscope (Figure 2b-d). Using dioxane as the good solvent, a single phase with a blue tint is observed after centrifugation, indicating nanoparticle formation. The optical microscopy image shown in Figure 2b is supportive of the sample forming nanoparticles as the first phase transition. Using a
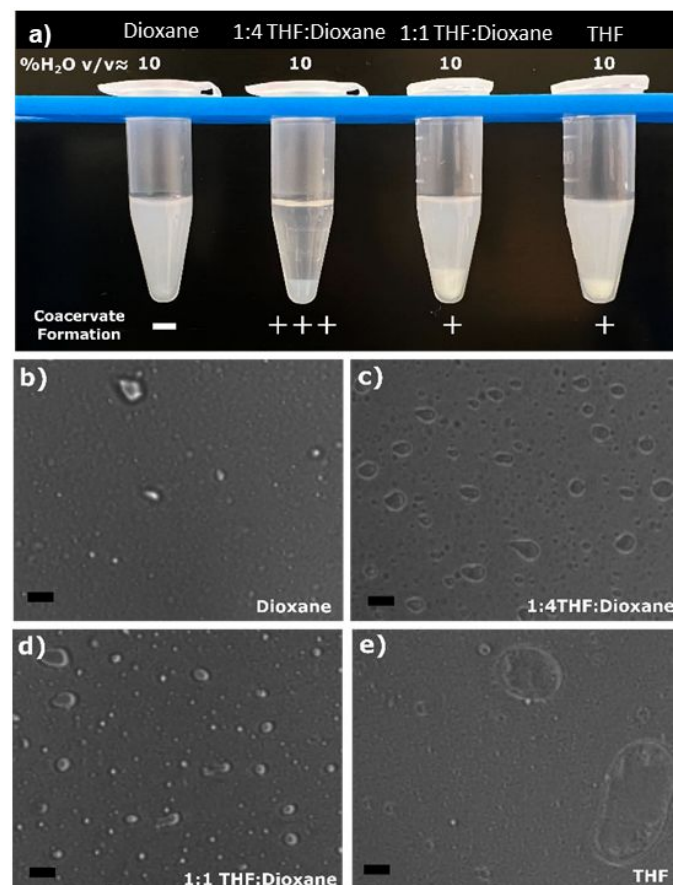

Figure 2. Phase behavior of PS_{200}-*b*-PAA_{35} in a series of "good" solvents. a) Photograph of PS_{200}-*b*-PAA_{35} in "good" solvents, titled above each sample, in critical concentrations of water. b) Optical microscopy of PS_{200}-*b*-PAA_{35} in dioxane showing no droplets. c) Optical microscopy of PS_{200}-*b*-PAA_{35} in 1:4 THF:dioxane showing most droplets. d) Optical microscopy of PS_{200}-*b*-PAA_{35} in 1:1 THF:dioxane showing a mixture of droplets and microparticles. e) Optical microscopy of PS_{200}-*b*-PAA_{35} in THF showing some droplets. The asymmetric/ellipsoidal appearance of droplets is due to the wetting of the glass substrates. Scale bars = 10 µm.

1:4 mixture of THF:dioxane as the good solvent, a dense layer of phase separated droplets upon centrifugation is observed. Optical microscopy of the dispersed sample revealed coacervate droplets as shown in Figure 2c. Furthermore, using a higher THF content of 1:1 THF:dioxane and 100% THF as the good solvents, a dense layer of droplets with a blue tinted top layer is observed after centrifugation, indicating a mixture of droplets and nanoparticles. The optical microscopy images also reveal the formation of micron size particles along with liquid-like droplets. (Figure 2a, d,&e). As we aim to compare the effect of LLPS and no LLPS during the solvent switch method, these last two systems with higher THF content were not further explored. Based on these studies, the two good solvent
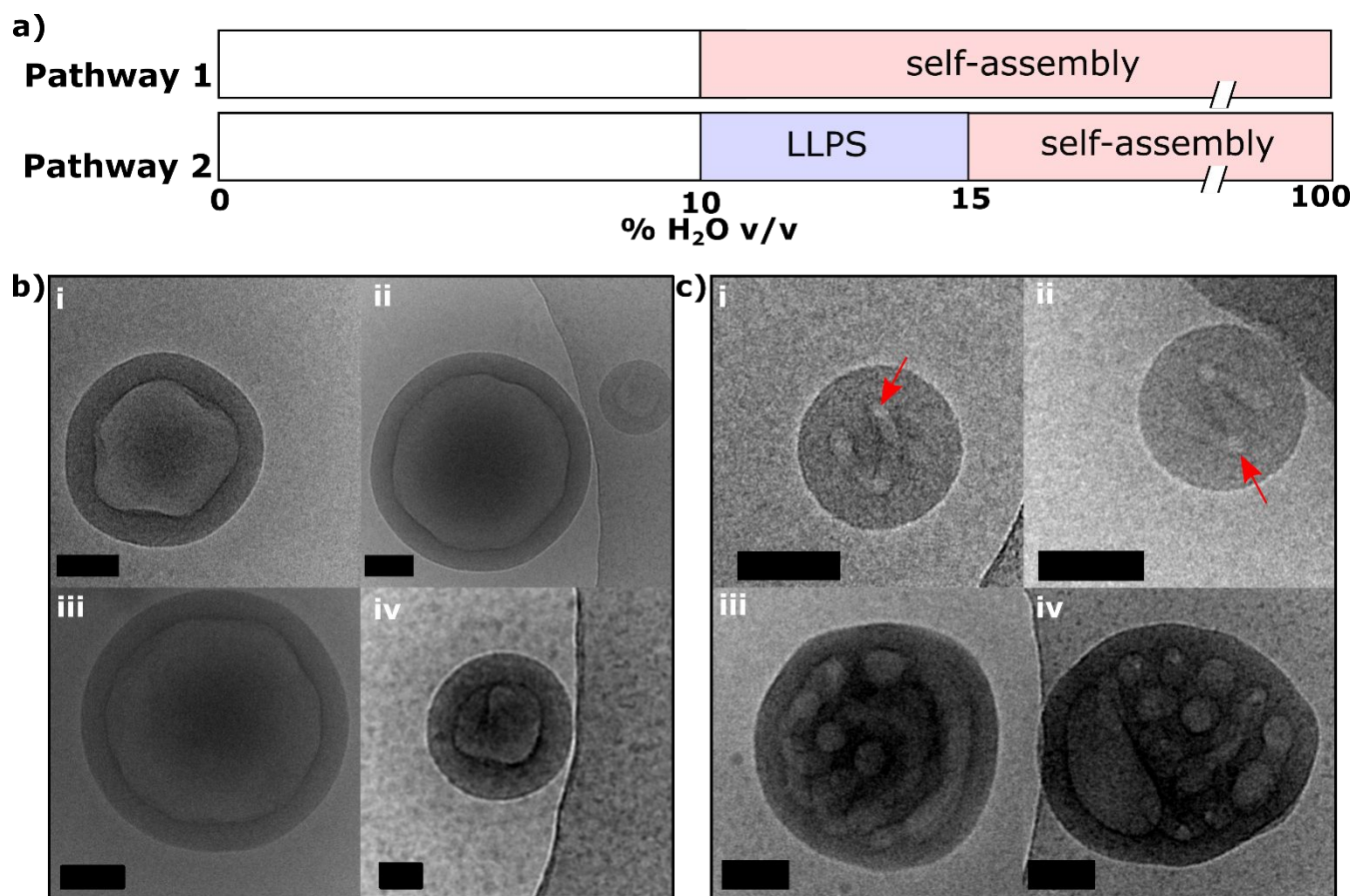
COMMUNICATION

Figure 3: LLPS and self-assembly of PS_{200}-b-PAA_{35}. a) Experimentally mapped phase trajectories of PS_{200}-b-PAA_{35} in dioxane (Pathway 1) and 1:4 THF:dioxane (Pathway 2), white indicates dissolved polymer, blue indicates coacervate formation, and red indicates self-assembled structures. b) Cryo-TEM images of PS_{200}-b-PAA_{35} vesicles assembled in system A. c) Cryo-TEM images of PS_{200}-b-PAA_{35} nanoparticle assembled in system B displaying a "confined" morphology of a sphere with a helical cavity as indicated by the red arrows, and waffle morphologies that were also present as the minor product. (Scale bars = 100 nm)

systems for our study are dioxane and 1:4 THF:dioxane which allow the polymers to assemble down Pathway 1 and 2 respectively, Figure 1.

To ensure we compare self-assembled particles for each of the systems, we mapped the phase trajectories for both pathways as shown in Figure 3a. Pathway 1 had no observed LLPS and Pathway 2 had a narrow range of water percentage where stable LLPS was observed (Supplementary Figure S1). The solvent switch experiments to compare the nanoparticles from each pathway were performed by dissolving the polymer in dioxane or 1:4 THF:dioxane. Water was then added dropwise using a syringe pump until the water concentration reached 50% v/v (Supplementary Figure S2). 50% v/v water ensures that both systems have reached the self-assembled regime, and subsequent reorganization of the nanoparticle morphologies should not occur due to kinetic trapping. The particles were then dialyzed against water for the complete removal of the organic solvents. CryoEM was performed on the dialyzed suspensions to determine the morphologies obtained from the different pathways. In the cryoEM images, the lighter regions correspond to solvated regions of the particles which contain the hydrated polyacrylic acid blocks. The darker regions correspond to

the desolvated polystyrene blocks. Pathway 1 exclusively forms vesicle structures with a mean diameter of 380 nm ± 125 nm and mean membrane thickness of 43 nm ± 4 nm, Figure 3b (n = 25, where n is the number of particles measured). Based on previous literature the vesicle morphology is expected from PS_{200}-b-PAA_{35} due its assymteric blocks and the packing parameter (see supplementary info).[36] In contrast, Pathway 2 forms two types of structures with complex internal features. The predominant morphology observed was spheres with helical cavities (80%) and mean diameters 200 nm ± 35 nm. A small population of particles were also observed with a waffle-like morphology (20%) and mean diameter 530 nm ± 100 nm, Figure 3c (n = 25). The formation of such structures by Pathway 2 was reproducible as tested by carrying out the self-assembly process in multiple batches (Figure S3). Previously, the formation of particles with helical cavities has only been explained by external spherical confinement of the block copolymers.[12,37] Using Monte Carlo simulations of block copolymers under spherical confinement, Chi et.al predicted a series of unconventional structures including spheres with internal helical cavities similar to the ones shown in Figure 3c.[37] While they were not studying LLPS in their systems, they do suggest these morphologies are only expected if the system undergoes confinement. This supports our hypothesis that LLPS

induces auto-confinement of block coplymers during the self-assembly process as we only observe spheres with helical cavites in Pathway 2. It is important to note that our previous work has shown that solvent switch systems with pathways that involve an LLPS precursor can also form vesicles.[28,29] Consequently, the observation of vesicles alone is not sufficient to determine between Pathway 1 vs Pathway 2. However, we believe the observation of morphologies such as helical cavities is good evidence of an auto-confinement based self-assembly process where EICA or SORP is not used.[37],[38] While the SORP method is well-established for driving the assembly of block copolymer particles, its potential for undergoing LLPS remains an unexplored avenue. Given the similarities in solvent dynamics between SORP and other methods where LLPS is observed, it's plausible that LLPS could also be an integral mechanism in the SORP process, meriting further investigation.

Studies on emulsion-based confinement indicate that evaporation rate directly impacts the morphologies of self-assembled structures.[10] It's plausible that this relationship also applies to LLPS-driven confinement, potentially explaining the variety of morphologies observed in self-assembled particles along pathway 2. Larger droplets will likely have a slower rate of solvent expulsion compared to smaller ones. Considering that the waffle like particles are approximately twice the size of the helical cavity spheres the difference in morphology could be a consequence of the different solvent expulsion rates from the precursor droplets as the size of the precursor droplet and formed particles are known to be directly related.[29]

In conclusion, our use of a model block copolymer system has successfully demonstrated the ability of block copolymers to engage in an auto-confinement driven self-assembly process, when LLPS is involved during the solvent switch procedure. More work will be required to understand the effect of different parameters, like "selective" solvent addition rates, block copolymer molecular weight, and concentration, on the LLPS induced auto-confinement. These results add to our understanding of how LLPS influences the self-assembly process of block copolymers. Furthermore, this study shows that LLPS precursors provide a rich landscape for controlling the size and morphology of block copolymer nanoparticles.[29] Lastly, the observations in this report opens up the possibility to study auto-confinement effects in other LLPS systems such as biological condensates.[39]

Supporting Information
Additional Microscopy and methods information is supplied as Supporting Information. Correspondence and requests for materials should be addressed to J.P.P.

References

[1] J. A. Moreno-Razo, E. J. Sambriski, N. L. Abbott, J. P. Hernández-Ortiz, J. J. de Pablo, *Nature* **2012**, *485*, 86–89.
[2] B. de Nijs, S. Dussi, F. Smallenburg, J. D. Meeldijk, D. J. Groenendijk, L. Filion, A. Imhof, A. van Blaaderen, M. Dijkstra, *Nat. Mater.* **2015**, *14*, 56–60.
[3] Y. Wu, G. Cheng, K. Katsov, S. W. Sides, J. Wang, J. Tang, G. H. Fredrickson, M. Moskovits, G. D. Stucky, *Nat. Mater.* **2004**, *3*, 816–822.
[4] S. Jun, B. Mulder, *Proc. Natl. Acad. Sci.* **2006**, *103*, 12388–12393.
[5] M. Pinot, F. Chesnel, J. Z. Kubiak, I. Arnal, F. J. Nedelec, Z. Gueroui, *Curr. Biol.* **2009**, *19*, 954–960.
[6] L. Shang, F. Ye, M. Li, Y. Zhao, *Chem. Soc. Rev.* **2022**, *51*, 4075–4093.
[7] G. Liu, A. J. Müller, D. Wang, *Acc. Chem. Res.* **2021**, *54*, 3028–3038.
[8] M. Wang, J. Li, G. Shi, G. Liu, A. J. Müller, D. Wang, *Macromolecules* **2021**, *54*, 3810–3821.
[9] A. M. Jimenez, A. S. Altorbaq, A. J. Müller, S. K. Kumar, *Macromolecules* **2020**, *53*, 10256–10266.
[10] K. H. Ku, Y. J. Lee, Y. Kim, B. J. Kim, *Macromolecules* **2019**, *52*, 1150–1157.
[11] Y.-T. Juan, Y.-F. Lai, X. Li, T.-C. Tai, C.-H. Lin, C.-F. Huang, B. Li, A.-C. Shi, H.-Y. Hsueh, *Macromolecules* **2023**, *56*, 457–469.
[12] F. Zhao, Z. Xu, W. Li, *Macromolecules* **2021**, *54*, 11351–11359.
[13] J. M. Shin, Y. Kim, K. H. Ku, Y. J. Lee, E. J. Kim, G.-R. Yi, B. J. Kim, *Chem. Mater.* **2018**, *30*, 6277–6288.
[14] D.-P. Song, T. H. Zhao, G. Guidetti, S. Vignolini, R. M. Parker, *ACS Nano* **2019**, *13*, 1764–1771.
[15] J. Hwang, S. Kim, U. Wiesner, J. Lee, *Adv. Mater.* **2018**, *30*, 1801127.
[16] C. K. Wong, X. Qiang, A. H. E. Müller, A. H. Gröschel, *Prog. Polym. Sci.* **2020**, *102*, 101211.
[17] T. Higuchi, A. Tajima, K. Motoyoshi, H. Yabu, M. Shimomura, *Angew. Chem. Int. Ed.* **2008**, *47*, 8044–8046.
[18] R. H. Staff, D. Schaeffel, A. Turshatov, D. Donadio, H.-J. Butt, K. Landfester, K. Koynov, D. Crespy, *Small* **2013**, *9*, 3514–3522.
[19] Q. Wang, A. Xiao, Z. Shen, X.-H. Fan, *Polym. Chem.* **2019**, *10*, 372–378.
[20] A. L. Parry, P. H. H. Bomans, S. J. Holder, N. A. J. M. Sommerdijk, S. C. G. Biagini, *Angew. Chem. Int. Ed.* **2008**, *47*, 8859–8862.
[21] H. Yu, X. Qiu, S. P. Nunes, K.-V. Peinemann, *Nat. Commun.* **2014**, *5*, 4110.
[22] N. S. Cameron, M. K. Corbierre, A. Eisenberg, **1999**, *77*, 16.
[23] S. F. Banani, H. O. Lee, A. A. Hyman, M. K. Rosen, *Nat. Rev. Mol. Cell Biol.* **2017**, *18*, 285–298.
[24] V. Yeong, J. Wang, J. M. Horn, A. C. Obermeyer, *Nat. Commun.* **2022**, *13*, 7882.
[25] M. H. Barbee, Z. M. Wright, B. P. Allen, H. F. Taylor, E. F. Patteson, A. S. Knight, *Macromolecules* **2021**, *54*, 3585–3612.
[26] T. Mashima, M. H. M. E. van Stevendaal, F. R. A. Cornelissens, A. F. Mason, B. J. H. M. Rosier, W. J. Altenburg, K. Oohora, S. Hirayama, T. Hayashi, J. C. M. van Hest, L. Brunsveld, *Angew. Chem. Int. Ed.* **2022**, *61*, e202115041.
[27] C. E. Sing, S. L. Perry, *Soft Matter* **2020**, *16*, 2885–2914.
[28] A. Ianiro, H. Wu, M. M. J. van Rijt, M. P. Vena, A. D. A. Keizer,

Soft Matter

A. C. C. Esteves, R. Tuinier, H. Friedrich, N. A. J. M. Sommerdijk, J. P. Patterson, *Nat. Chem.* **2019**, *11*, 320–328.

[29] A. Rizvi, U. Patel, A. Ianiro, P. J. Hurst, J. G. Merham, J. P. Patterson, *Macromolecules* **2020**, *53*, 6078–6086.

[30] A. Rizvi, J. T. Mulvey, J. P. Patterson, *Nano Lett.* **2021**, *21*, 10325–10332.

[31] C. K. Wong, M. Heidelmann, M. Dulle, X. Qiang, S. Förster, M. H. Stenzel, A. H. Gröschel, *J. Am. Chem. Soc.* **2020**, DOI 10.1021/jacs.0c02009.

[32] Y. Mai, A. Eisenberg, *Chem. Soc. Rev.* **2012**, *41*, 5969–5985.

[33] D. E. Discher, A. Eisenberg, *Science* **2002**, *297*, 967–973.

[34] A. Choucair, A. Eisenberg, *Eur. Phys. J. E Soft Matter* **2003**, *10*, 37–44.

[35] L. Chen, H. Shen, A. Eisenberg, *J. Phys. Chem. B* **1999**, *103*, 9488–9497.

[36] P. Lim Soo, A. Eisenberg, *J. Polym. Sci. Part B Polym. Phys.* **2004**, *42*, 923–938.

[37] P. Chi, Z. Wang, B. Li, A.-C. Shi, *Langmuir* **2011**, *27*, 11683–11689.

[38] J.-P. Xu, J.-T. Zhu, *Chin. J. Polym. Sci.* **2019**, *37*, 744–759.

[39] S. Boeynaems, S. Alberti, N. L. Fawzi, T. Mittag, M. Polymenidou, F. Rousseau, J. Schymkowitz, J. Shorter, B. Wolozin, L. V. D. Bosch, P. Tompa, M. Fuxreiter, *Trends Cell Biol.* **2018**, *28*, 420–435.